

New techniques for chargino-neutralino detection at LHC

Maria Eugenia Cabrera

*University of Amsterdam
Institute of Theoretical Physics
GRAPPA
E-mail: M.E.CabreraCatalan@uva.nl*

J. Alberto Casas

*Instituto de Física Teórica, IFT-UAM/CSIC
U.A.M., Cantoblanco,
28049 Madrid, Spain
E-mail: alberto.casas@uam.es*

Bryan Zaldivar

*Instituto de Física Teórica, IFT-UAM/CSIC
U.A.M., Cantoblanco,
28049 Madrid, Spain
E-mail: b.zaldivar.m@csic.es*

ABSTRACT: The recent LHC discovery of a Higgs-like boson at 126 GeV has important consequences for SUSY, pushing the spectrum of strong-interacting supersymmetric particles to high energies, very difficult to probe at the LHC. This gives extra motivation to study the direct production of electroweak particles, as charginos and neutralinos, which are presently very poorly constrained. The aim of this work is to improve the analysis of chargino-neutralino pair production at LHC, focusing on the kinematics of the processes. We propose a new method based on the study of the *poles* of a certain kinematical variable. This greatly improves the low-statistics problems associated with other approaches based on the study of end-points. We illustrate the method with particular SUSY models, and show that working with the LHC at 100/fb luminosity one would be able to distinguish the SUSY signal from the Standard Model background.

KEYWORDS: [Beyond Standard Model](#), [Collider physics](#), [Supersymmetry Searches](#), [Kinematic Variables](#), [LHC physics](#), [chargino neutralino production](#).

Contents

1. Introduction	1
2. State of the art of the analysis	3
3. Our Strategy	4
3.1 The visible transverse energy	4
3.2 From CM to LAB	5
4. Testing the efficiency of E_T^v and p_T^v in concrete SUSY models	9
5. Conclusions	14

1. Introduction

The recent discovery of the Higgs boson, with a mass around 126 GeV [1], [2], does not only have crucial importance by itself. It also has far-reaching consequences for well-motivated candidates for physics beyond the Standard Model (SM), such as Supersymmetry (SUSY), and in particular the Minimal Supersymmetric Standard Model (MSSM).

As it is well-known, in the MSSM the tree-level Higgs-mass in the MSSM is bounded by the mass of the Z -boson, so large radiative corrections are needed in order to reconcile theory and experiment. These corrections go with (the logarithm of) the supersymmetric masses, in particular with the stop masses. Consequently, these masses must be rather high (well above 1 TeV unless there are unlikely conspiracies) in order to reconcile the theory with the experimental Higgs mass. This means that the MSSM is in trouble. First of all, such large supersymmetric masses are in tension with the naturalness of the electroweak breaking. But, beyond naturalness considerations, large supersymmetric masses imply that the MSSM is going to be difficult to test at the LHC.

In constrained versions of the MSSM, such as the popular constrained MSSM (CMSSM), the stop masses are directly related to the universal scalar mass, m_0 , and gaugino mass, $m_{1/2}$ at the high scale. So large stop masses imply also large squark and gluino masses. Actually, the lower bounds for these physical masses are beyond the present (and most probably the future) LHC reach []. In other words, even if the MSSM is true, $m_h \simeq 126$ GeV implies that it will be difficult to discover it at the LHC studying the production and decay of squarks and gluinos, which has been so far the golden channel of potential SUSY production. Going beyond the CMSSM does not help much, as the values of the physical stop masses are directly related to the stop and gluino initial masses (due to the coupled renormalization-group running). Still, one could have heavy stops and light first and second generation squarks, though this possibility is rather strange from the theoretical point

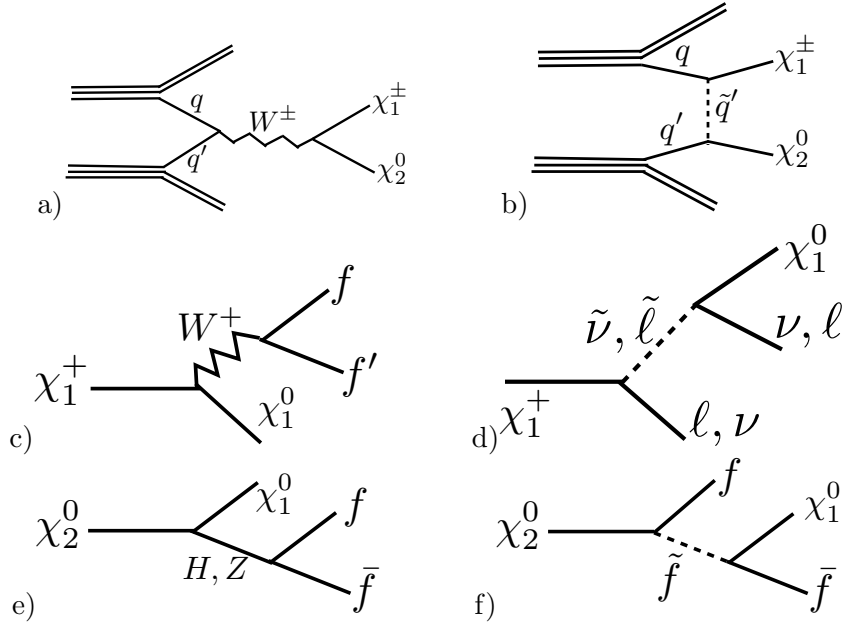


Figure 1: a) and b) Typical production processes of a pair $\chi_1^\pm \chi_2^0$ in the LHC. c) and d) Chargino decay modes. e) and f) Neutralino decay modes.

of view. On the other hand, the production of supersymmetric particles with no strong interactions may become one of the most promising possibilities to detect SUSY, especially in non-constrained MSSM models.

The latter is an important motivation to explore chargino-neutralino production and detection at the LHC. Actually, relaxing the severe universality of the CMSSM (in particular for the gaugino sector), one can have relatively light charginos and neutralinos, while still having squarks and gluinos very heavy. On the other hand, charginos and neutralinos can produce not only hadronic, but also purely leptonic final states, with distinctive features which make them very attractive.

Another motivation comes from dark matter (DM) constraints. The last data of XENON100 in combination with the Higgs mass have narrowed enormously the MSSM candidates for DM. Probably the most satisfactory scenario that survives occurs when the lightest neutralino is pure Higgsino with a mass around 1 TeV. But if gaugino masses are not universal it is also possible to have a much lighter (pure bino) neutralino which annihilates in the early universe through a combination of Z -boson and Higgs funnels.

In summary, a scenario where all the supersymmetric particles are too heavy, except charginos and neutralinos is plausible and has phenomenological motivations. Therefore it would be worth to improve the present techniques to analyze the production and detection of chargino/neutralino pairs at the LHC; and this is the main motivation of this paper.

In the most of the cases the chargino-neutralino pair is $\chi_1^\pm \chi_2^0$, i.e. the lightest chargino and the next-to-lightest neutralino. The corresponding diagrams of production and decay are shown in fig.(1). The chargino and the neutralino can decay in several ways, always giving an LSP (χ_1^0) at the end of each cascade.

The study of chargino-neutralino pair production has been performed previously in [3], [4], through the analysis of leptonic final states. The aim of our work is to improve those analyses, by proposing new strategies which are complementary and more efficient in some cases. Our analysis is by construction independent of the diagram through which the chargino and the neutralino decay, since it is entirely based on the properties of the final states. It can also be applied to hadronic final states, such as $b\bar{b}\ell$.

The outline of the paper is as follows. In section 2 we describe the present status of the analyses of possible chargino-neutralino production and detection, as done by ATLAS and CMS groups, and motivate the need to improve this kind of analysis. In section 3 we describe our strategy, by proposing a kinematical variable which allows to obtain direct information about the SUSY spectrum. It is also very useful to concentrate signal-events, thus improving the S/B ratio and the LHC potential for discovery of new physics. Section 4 is devoted to illustrate the use of this variable in concrete SUSY models, showing its advantages with respect to other variables (**esto ultimo no estoy seguro de que lo hagamos**). We finally conclude in section 5.

2. State of the art of the analysis

As shown in fig.(1), the neutralino χ_2^0 can decay through a sfermion¹, a sneutrino, a Higgs or a Z -boson, depending on the kinematical availability and the χ_2^0 composition. Likewise, the chargino χ_1^\pm can decay, among other channels, through a sfermion, a sneutrino or a W -boson. If χ_1^\pm and χ_2^0 decay through right-handed (left-handed) sleptons², the final state will contain $3\ell + \nu$ ($\ell + 3\nu$), plus the two χ_1^0 neutralinos. However, as long as the sleptons are heavier than χ_2^0 and χ_1^\pm , these decay channels become very suppressed and the decays through on-shell Higgs, Z and W dominate.

Ref. [3] contains a study of purely leptonic final states of the type $\ell^+\ell^-\ell'^\pm$, where ℓ and ℓ' may be identical leptons. The authors perform separate analyses of two cases: 1) the invariant mass of identical opposite-sign leptons ($m_{\ell+\ell^-}$) does *not* reproduce the Z -boson mass, M_Z , and 2) it does. They assume that the χ_2^0 decays through a slepton (case 1) or a Z -boson (case 2). In both cases, they use the E_T^{miss} variable to compare the actual experimental data with the SM background, finding no significant excess of events, once all the uncertainties are taken into account. The negative result is then interpreted as contour bounds in the parameter space of e.g. concrete simplified models.

A more complete analysis was presented later in ref.[4]. Again, the authors focus on 3-lepton final states, but using the variable E_T^{miss} or $m_{\ell+\ell^-}$ in combination with M_T , i.e. the transverse mass built with the momentum of the unpaired lepton and E_T^{miss} . One option gives better sensitivity than the other, depending on the mass splittings between χ_1^0 and its respective mothers. A second analysis was performed for 2-lepton final state, considering the possibility that one of the 3 leptons produced by χ_1^\pm or χ_2^0 may be lost or

¹For the purposes of this discussion we call “sfermions” all the charged fermion superpartners, separating them from sneutrinos.

² $\nu_R, \tilde{\nu}_R$ are not considered in this analysis.

does not pass the kinematical cuts. In a last analysis they considered that both χ_1^\pm and χ_2^0 may decay through on-shell vector bosons, giving $2\ell + 2j$ in the final state, for which the SM background has not intrinsic E_T^{miss} . Using these techniques they were able to provide contour bounds on χ_1^\pm, χ_2^0 and χ_1^0 masses for particular simplified models.

A quite efficient analysis of the decay through sleptons was presented in ref. [5], where the authors used the $m_{\ell+\ell^-}$ variable. An obvious advantage of this choice is that $m_{\ell+\ell^-}$ is Lorentz invariant and thus the analysis is fully valid in the (boosted) LAB frame. It can be shown that, when the intermediate leptons are produced on-shell, the histogram on $m_{\ell+\ell^-}$ has an edge for $m_{\ell+\ell^-}|_{\text{edge}} = f(M_{\chi_2^0}, M_\chi, m_\ell)$, where f is a certain combination of the χ_2^0, χ_1^0 and ℓ masses. When the leptons are produced off-shell, the authors use a strategy based on the study of end-points in m_{l+l^-} . This can be, however, pretty inefficient, since by definition one has poor statistics and a difficult-to-control background.

Note that most of the previous analyses either do not provide direct information about the relevant SUSY spectrum or are quite inefficient due to poor statistics (with the exception of the χ_2^0 -decay through on-shell sleptons based on $m_{\ell+\ell^-}$). In addition, they are designed to work for specific channels of decay (through sleptons or Z -boson).

In this paper we propose the use of a variable whose distinctive feature is to concentrate the signal events around a peak, not relying on edges nor end-points, and allowing to access directly to information about the spectrum. Besides, it can be applied without any assumption or guess about the decay mode that takes place (through Z -boson, sleptons, Higgs or whatever). We describe the idea in the next section.

3. Our Strategy

3.1 The visible transverse energy

In contrast with the previous analyses, our strategy is purely kinematical and based only on the characteristics of the initial (χ_2^0) and the final states ($f\bar{f}\chi_1^0$); so it is independent of the channel through which the χ_2^0 decays. As it is based just on the χ_2^0 -chain, the analysis can be easily combined with other analyses that use partial information from both the χ_2^0 and the χ_1^\pm chains. It can also be applied to other processes where one or two χ_2^0 states are produced.

We initially work in the reference frame in which χ_2^0 is at rest, which we call CM (do not confuse with the center-of mass of the partonic collision) and consider the \mathcal{E}_T variable, defined as

$$\mathcal{E}_T = \hat{E}_T^v + \hat{E}_T^\chi \quad (3.1)$$

where $\hat{E}_T^v, \hat{E}_T^\chi$ are the transverse energies of the the visible system (e.g. $v \equiv \ell^+\ell^-$) and the missing system,

$$\hat{E}_T^v = \sqrt{M_v^2 + (\hat{p}_T^v)^2}, \quad \hat{E}_T^\chi = \sqrt{M_\chi^2 + (\hat{p}_T^\chi)^2} \quad (3.2)$$

Here M_v and M_χ are the invariant masses of the visible system and the LSP (χ_1^0) and the hats denote CM quantities everywhere. Of course, $(\hat{p}_T^v)^2 = (\hat{p}_T^\chi)^2 \equiv p_T^2$.

As it has been discussed in ref. [6], the histogram of events displayed in the \mathcal{E}_T variable has a pole at the mass of χ_2^0 ,

$$\mathcal{E}_T|_{\text{pole}} = E_{\text{CM}} = M_{\chi_2} \quad (3.3)$$

Besides, for $\mathcal{E}_T > M_2$ there are no events, so the histogram has an sharp edge at the pole. Hence, potentially, the \mathcal{E}_T variable can give a very distinctive signal, well separated from the background, providing in addition direct information about the SUSY spectrum. Note also that \mathcal{E}_T is invariant under longitudinal boosts. There are however some problems. First, even working at the CM frame, i.e. assuming that χ_2^0 was produced with vanishing transverse momentum, we cannot measure the invisible transverse energy, E_T^χ , due to the uncertainty on M_χ , which normally is not negligible. We have checked that in general $M_\chi \simeq 0$ is not a good approximation. Second, the χ_2^0 neutralino is usually produced with a non-vanishing transverse momentum. We postpone the second issue to the next subsection and focus now on the first one.

In order to avoid the dependence on unknown quantities, a good strategy is to work just with the visible transverse energy, E_T^v , defined in eq.(3.2). It can be easily checked that the pole in the \mathcal{E}_T variable, eq.(3.3) translates into a pole in \hat{E}_T^v ,

$$\hat{E}_T^v|_{\text{pole}} = \frac{1}{2M_{\chi_2}} [M_{\chi_2}^2 - M_\chi^2 + M_v^2] \quad (3.4)$$

In general, the mass of the visible system, M_v , can change from event to event. However, if χ_2^0 decays through a Higgs (very common case) or through a Z -boson, all the events are concentrated around $M_v = m_h$ (M_Z). An example of this kind, which shows clearly the edge and pole in the CM frame can be seen in the plot a) of Fig.2, to be discussed below in more detail. When χ_2^0 decays through sleptons, we can select a fraction of the events with similar M_v , and check that in CM a pole appears as in (3.4). This decreases the statistics but not in a dramatic way. Actually, in cases where $M_v^2 \ll M_{\chi_2}^2$, one could do a histogram with all the events, since the pole appears then around $\hat{E}_T^v \simeq \frac{1}{2M_{\chi_2}}(M_{\chi_2}^2 - M_\chi^2)$. Next, we study what happens when we go from the CM to the actual LAB frame.

3.2 From CM to LAB

The clean and sharp behavior of the \hat{E}_T^v variable in CM becomes of course less keen-edged when passing to the LAB frame. This is illustrated by the plots of Fig. 2. They correspond to a CMSSM model with $m_0 = 500$ GeV, $M_{1/2} = 700$ GeV, $\tan \beta = 10$, $A_0 = 0$, and $\mu > 0$. The relevant spectrum for us is $M_{\chi_2} \approx 554$ GeV and $M_\chi \approx 294$ GeV. The χ_2^0 neutralino decays almost entirely through an on-shell Higgs. In the CM frame the pole for E_T^v is at ~ 210 GeV. We have simulated the events using `Pythia`, with a center-of-mass energy $\sqrt{s} = 7$ TeV and a luminosity of 20/fb. The upper (lower) plots of Fig.2 correspond to events where the Higgs decayed into $\tau\bar{\tau}$ (a pair of b-jets, $j_b j_b$). The left (right) plots are obtained in the CM (LAB) frame. We emphasize that this example is just for illustrative purposes. For this reason we have not incorporated a realistic τ -reconstruction, as well as b-jet identification.

As expected, the CM histograms show a very clear and sharp peak (pole) around 200–220 GeV, followed by an edge. In the case of the $j_b j_b$ histogram there appear events

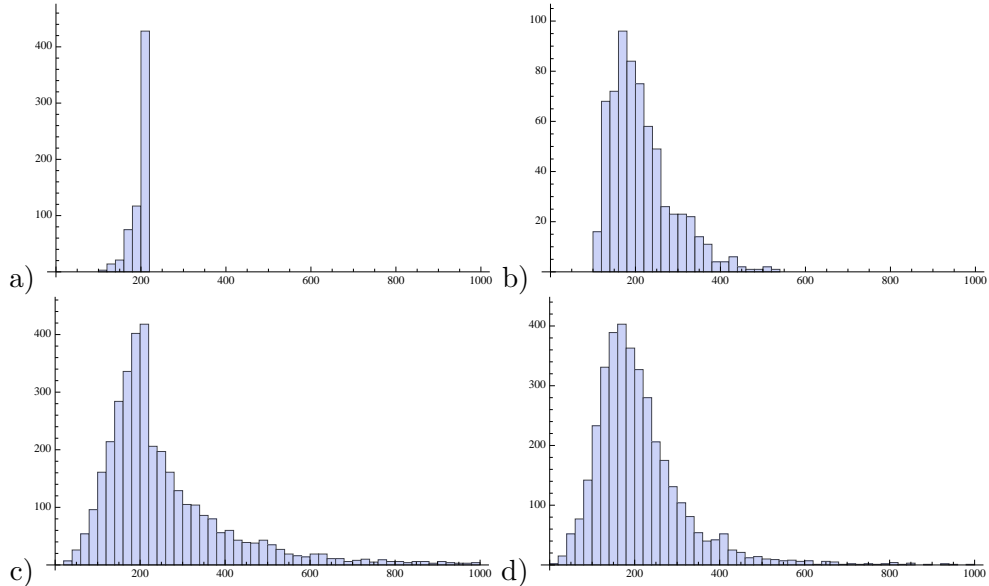


Figure 2: Histogram (number of events) of E_T^v in the cases where v is a) a $\tau\bar{\tau}$ pair in the CM frame; b) a $\tau\bar{\tau}$ pair in the LAB frame; c) a jj pair in the CM frame, and d) a jj pair in the LAB frame. The details of the SUSY point correspondent to this histograms are described in the text.

beyond the edge due to the limited efficiency in the jet reconstruction. The corresponding LAB histograms show two (non-dramatic) differences. First, a logical spreading around the maximum; and second, a slight shift of the peak towards smaller values of E_T^v . This shift is almost invisible for the $j_b j_b$ histogram. All these effects can be explained, estimated in a semi-analytical way and kept under control, as we discuss below.

We recall that the transverse variables we are using are only affected by transverse boosts when passing from CM to LAB. Longitudinal boosts are irrelevant for this analysis. There are two sources of transverse boosts. First, the partonic collision will not occur in general in the center-of-mass, i.e. it will have a non-vanishing net transverse momentum, typically due to initial state radiation. Second (and more importantly) even at the center-of-mass of the partonic collision, χ_2^0 can be produced with non-vanishing transverse momentum (and opposite to that of χ_1^\pm). Next we estimate the change in the E_T^v of the events at the pole due to the non-vanishing transverse momentum of χ_2^0 in the LAB.

We will distinguish two perpendicular directions in the transverse plane: the direction along $p_T^{\chi_2}$ (\parallel), and the perpendicular to it (\perp). Due to the boost in the \parallel direction (we will ignore the boost in the longitudinal direction, which is irrelevant here), the visible energy changes (from CM to LAB) as

$$\hat{E}^v \rightarrow E^v = \gamma \hat{E}^v - \beta \gamma (\hat{p}_T^v)_\parallel \quad (3.5)$$

where $(\hat{p}_T^v)_\parallel$ is the component of the visible 3-momentum in the \parallel direction. As usual, γ and β are the parameters of the Lorentz transformation, satisfying

$$\beta \gamma = \frac{|p_T^{\chi_2}|}{M_{\chi_2}}. \quad (3.6)$$

Now, for the events in the pole $\hat{E}_T^v = \hat{E}_v$ in the CM frame [6], which holds after the transverse boost. Hence, when going to LAB, for those events the transverse energy changes as in eq.(3.5):

$$\hat{E}_T^v \rightarrow E_T^v = \gamma \hat{E}_T^v - \beta \gamma (\hat{p}_T^v)_\parallel \quad (3.7)$$

which represents a shift

$$\Delta \hat{E}_T^v = (\gamma - 1) \hat{E}_T^v - \beta \gamma (\hat{p}_T^v)_\parallel . \quad (3.8)$$

Let us estimate the size of this shift. Since for a non-relativistic boost, $\gamma - 1 \simeq \frac{1}{2} \beta^2 \gamma^2$, the second term in the r.h.s. of (3.8) will normally be the dominant one, because it scales as β instead of β^2 . However this term represents a shift, which sometimes is positive and sometimes negative (depending on the sign of β), whereas the first term, which scales as β^2 , is always positive. On the other hand, in average, $(\hat{p}_T^v)_\parallel \sim \frac{1}{\sqrt{2}} \hat{p}_T^v$. Using eq.(3.4) we can express \hat{p}_T^v as a combination of the masses involved in the system,

$$(\hat{p}_T^v)_\parallel^2 \Big|_{\text{pole}} = \frac{1}{4M_{\chi_2}^2} [M_{\chi_2}^2 - M_\chi^2 + M_v^2]^2 - M_v^2 . \quad (3.9)$$

This gets simplified when $M_v^2 \ll M_2^2$, e.g. when the decay occurs via Higgs or Z -boson and also in the other cases if we select events with relatively small M_v . Therefore, at the pole

$$(\hat{p}_T^v)_\parallel \simeq \frac{1}{\sqrt{2}} \frac{1}{2M_{\chi_2}} (M_{\chi_2}^2 - M_\chi^2) \simeq \frac{1}{\sqrt{2}} \hat{E}_T^v \Big|_{\text{pole}} , \quad (3.10)$$

which substituted back in eq.(3.8) gives

$$\Delta \hat{E}_T^v \simeq \left(\frac{1}{2} \beta^2 \gamma^2 - \frac{1}{\sqrt{2}} \beta \gamma \right) \hat{E}_T^v . \quad (3.11)$$

We recall that this expression is valid for events lying at the pole, which of course are especially interesting as they provide the maximum in the histogram of the signal. Now for a numerical evaluation of $\Delta \hat{E}_T^v$ we need to estimate $\beta \gamma$. It can be empirically checked that typically the transverse momentum of χ_2^0 is in average

$$|p_T^{\chi_2} | \simeq \frac{1}{3} M_{\chi_2} \quad (3.12)$$

and this value gets slightly smaller as M_2 increases. Actually this is consistent with expectations. First, the production of $\chi_1^\pm \chi_2^0$ through a W in S -channel (see Fig.1a) is dominated by the resonance. Although the W will be normally off-shell, the penalisation for large momenta of $\chi_1^\pm \chi_2^0$ is important, although this reason becomes weaker for $M_W \ll M_{\chi_2} + M_{\chi_1^\pm}$. Second, and more importantly, the PDFs penalize large energies. Since the final state particles are colourless (in this case charginos and neutralinos) with a net charge, they are essentially produced via quarks/antiquarks (and not gluons). This is significantly affected by the anti-quarks PDFs, which tend to prefer lower momenta rather than higher ones. As a consequence of these two effects, the final state particle energies are expected to be very close to their mass. This is consistent with the relation (3.12), which implies that the

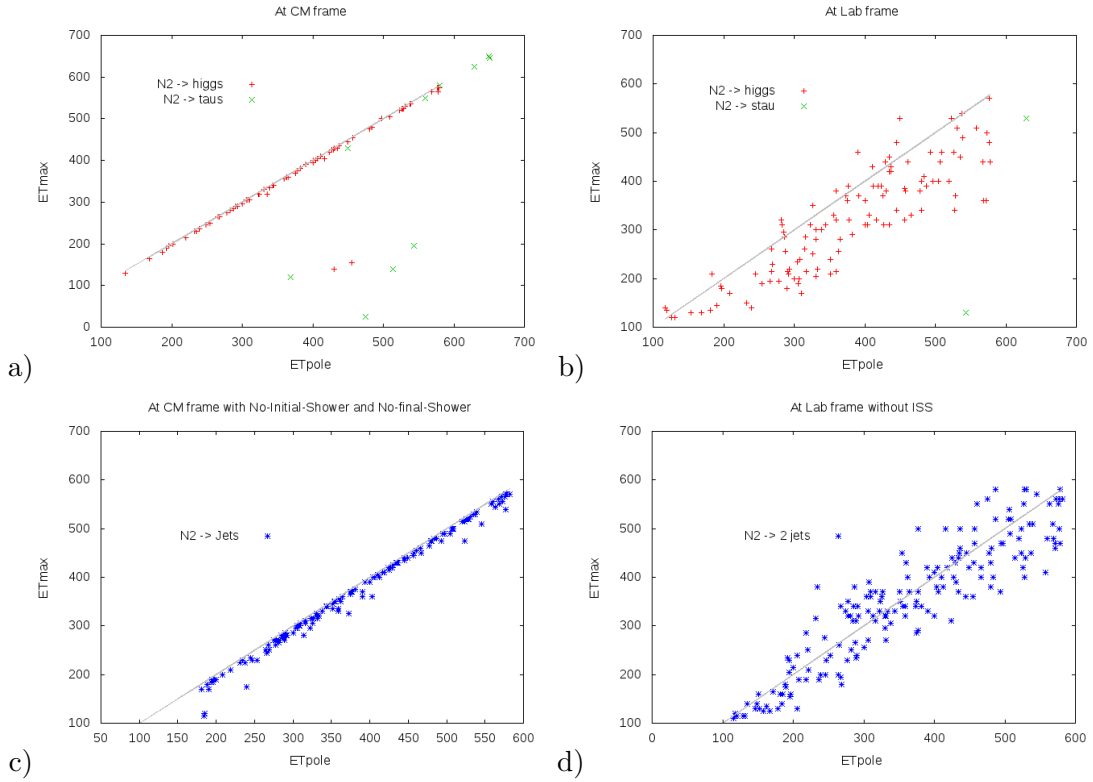


Figure 3: Scatter plot of different SUSY models showing the correlation between $E_T^v|_{\text{pole}}$ and the peak value of the variable E_T^v , reconstructed event by event for each point. This is done for the cases: a) $\tau\bar{\tau}$ pair in the CM frame; b) $\tau\bar{\tau}$ pair in the LAB frame; c) jj pair in the CM frame, and d) jj pair in the LAB frame. For the plot correspondent to taus, the green points show SUSY models where the neutralino χ_2^0 decayed through $\tilde{\tau}$ instead of H .

energy of the particle produced differs less than 5% from its mass. In consequence, from eq.(3.6) typically $\beta\gamma \simeq 1/3$. Then:

$$\Delta\hat{E}_T^v = \left(\frac{1}{18} \pm \frac{1}{3\sqrt{2}} \right) \hat{E}_T^v, \quad (3.13)$$

where we have already incorporated the fact that β has a random sign. This implies a shift $[-0.18 - 0.29] \hat{E}_T^v$ in the visible transverse energy of the pole events. Finally, we have to evaluate how this modifies the position of the peak. Notice that the pole events shifted positively (to the right of the histogram), will not produce any new global maximum as they fall in a region of E_T^v where there were almost no events. On the other hand the pole events shifted negatively (to the left of the histogram) will populate a region where there were already events. In addition, that region gets also populated by positive shifts of non-pole events, with lower \hat{E}_T^v values. Consequently, we expect a maximum in a value of E_T^v which is approximately 18% smaller than the value of the pole in CM, see eq.(3.4).

Fig.3 shows scatter plots of large set of SUSY models, showing the correlation between the theoretical $\hat{E}_T^v|_{\text{pole}}$, given by eq.(3.4), and the actual peak value of the E_T^v -histogram, reconstructed for each SUSY model. The upper (lower) plots correspond to histograms of

events where the χ_2^0 neutralinos decayed into a $\tau\bar{\tau}$ - ($j_b j_b$ -) pairs. We remark again that these plots are shown for illustrative purposes only, so no attempt of realistic identification of the τ and b -jets states is done at this level³. The left (right) plots correspond to histograms in the CM (LAB) system. The CM plots show the perfect correlation of the histogram maximum and the theoretical pole (3.4). The LAB plots show the two effects expected: a certain spreading and a net shift of the average maximum with respect to the CM prediction (straight lines). More precisely, the results for $\tau\bar{\tau}$ events are consistent with the previously discussed $\Delta\hat{E}_T^v \simeq -18\%\hat{E}_T^v$ expectation. It is remarkable, however, that for $j_b j_b$ events, the LAB results are more symmetrically distributed around the CM prediction. This can be easily understood by recalling that for $j_b j_b$ events the CM histogram does not have an end-point at the pole because of the limited efficiency in the jet reconstruction, see plot c) of Fig.2. In consequence the discussion after eq.(3.13) gets now modified since for the pole $j_b j_b$ -events shifted positively fall in a region of E_T^v where there were already events. In consequence, the limited efficiency in the jet reconstruction funnily makes the position of the maximum more stable than for leptonic histogram; thus the symmetric spreading of the LAB scatter-plot around the CM prediction.

One of the most interesting features of the E_T^v variable is that it concentrates the signal events around a maximum (determined by the supersymmetric spectrum), which does not happen for the background events (these get concentrated around M_Z , see below). This behavior is extremely helpful to separate the signal events from the background events, thus improving the signal/background (S/B) ratio in the search of new physics at LHC (even before using this variable to extract information about the SUSY spectrum). It should be noticed here that the background events (typically SM production of WZ) behave as if the "neutralino" χ_2^0 had exactly the mass of the Z -boson and the "neutralino" χ_1^0 had zero-mass. Thus for the background events the peak in the E_T^v variable lies at $\sim M_Z$.

For some SUSY models, however, the position of the maximum of the signal -determined by eq.(3.4)- can be close to M_Z , i.e. the peak of E_T^v for background events. Then, the strategy to detect the existence of new-physics-signal events can be further improved by plotting the p_T^v variable rather than E_T^v (of course, both variables are equivalent since they are unambiguously related through $E_T^v = \sqrt{M_v^2 + (p_T^v)^2}$, where M_v is a measurable quantity). Note that for the background events, the peak in p_T^v is at zero (in practice, close to the lower kinematical cut used), while for the signal events is given by eq.(3.9), and lies normally at some non-trivial value (even if the corresponding E_T^v is close to M_Z). In the next section we will see some explicit examples where the use of the p_T^v variable is very convenient to show the existence of new physics in the first place. Once, the new physics is detected, the value of p_T^v at the maximum of the signal can be related to the SUSY spectrum through eq.(3.9) or equivalently through eq.(3.4).

In the next section we explore these features in further detail.

4. Testing the efficiency of E_T^v and p_T^v in concrete SUSY models

As we have described before, the chargino-neutralino pair production can be studied

³In this sense, a more realistic analysis is performed in the next subsection

through the use of the visible transverse energy, E_T^v , regardless of the way the neutralino χ_2^0 has decayed. So here we only care about initial and final states.

We will simulate LHC signals with $\sqrt{s}=14$ TeV and luminosity of 100/fb, using the codes `SuSpect`, `HDECAY` and `SDECAY`⁴ as well as `SOFTSUSY`[11] for the spectrum calculators, and `MadGraph` /`MadEvent` [12] and `PYTHIA`[13] for the event simulation. We focus on events with 3 leptons + missing transverse momentum, and apply the following general cuts

- the existence of at least two identical, opposite signed leptons
- the 3rd hardest lepton having $E_T > 10$ GeV⁵
- The transverse mass of the 2nd chain $M_T > 90$ GeV,⁶
- Jet veto
- PGS cuts

We illustrate our strategy by working in the context of the MSSM. Specifically we choose the following SUSY models (defined at the M_{susy} scale)

$$\begin{aligned}
\text{Model 1 :} & \quad M_1 \simeq 99.8 \text{ GeV}, \quad M_2 \simeq 183.8 \text{ GeV}, \quad \mu \simeq 705, \quad \tan \beta = 10, \\
\text{Model 2 :} & \quad M_1 \simeq 47.2 \text{ GeV}, \quad M_2 \simeq 244.1 \text{ GeV}, \quad \mu \simeq -515.4, \quad \tan \beta = 19, \\
\text{Model 3 :} & \quad M_1 \simeq 93.9 \text{ GeV}, \quad M_2 \simeq 405.4 \text{ GeV}, \quad \mu = -5372.4, \quad \tan \beta = 50
\end{aligned}
\tag{4.1}$$

where M_1, M_2 are the first and second gaugino masses at low-energy, and $\tan \beta \equiv \langle H_u \rangle / \langle H_d \rangle$ is the ratio between the VEVs of the two Higgs doublets. We do not specify the values of gluino and sfermion masses, which are assumed to be heavy (note that we are not imposing gaugino-mass unification). In the three models we study the signal of χ_2^0 decaying through a Z -boson, which is the dominant one for all of them (more details below).

The strategy of the analysis for the three models is the following:

- We reconstruct the possible invariant masses M_v of a pair of identical leptons, selecting the events where a pair of opposite-sign leptons has an invariant mass close to M_Z

$$M_v = m_Z \pm 10 \text{ GeV},$$

This pair is identified as a daughter of a Z , thus the third lepton, ℓ' , should come from a W . This holds for both the signal and the SM WZ background.

It is important to note that most of the WZ background events are actually extracted thanks to the $M_T > 90$ GeV requirement in the above list of cuts. The reason is the following. Taking into account that for the events of the background the

⁴all included in a single package called `SUSY-HIT` [7, 8, 9, 10].

⁵This is for electrons. For muons, the same cut is applied on its p_T instead.

⁶Computed with the unpaired lepton, see discussion below.

missing momentum can be identified with the neutrino, one constructs the associated transverse mass, which satisfies the following inequality

$$(M_T^{\ell'\nu})^2 = (E_T^{\ell'} + E_T^\nu)^2 - (\vec{p}_T^{\ell'} + \vec{p}_T^\nu)^2 \leq M_W^2, \quad (4.2)$$

where ℓ' is the charged lepton coming from the W (i.e. the unpaired lepton). Hence, identifying p_T^{miss} with p_T^ν and discarding events with $M_T^{\ell'\nu} > M_W$ would in principle extract the whole WZ background. Although, due to the inefficiency in the reconstruction of the missing piece, some background events may violate in practice the inequality (4.2), this turns out to be an extremely efficient constraint to improve the S/B ratio.

- With the surviving events, we reconstruct the E_T^v , p_T^v variables associated to the lepton pair daughter of the Z .
- We simulate the background taking into account only the contribution from WZ production, which is by far the dominant one in the regions of interest (see e.g. [3]). We have checked that the results of our simulations are in agreement with [3].
- Finally, we construct the E_T^v , p_T^v histograms and study the size of the signal over the background.

Next we expound the results obtained for the three models considered, in a separate way.

Model 1

From the initial parameters listed in eq.(4.1), we obtain the relevant supersymmetric spectrum for the analysis, which reads

$$M_{\chi_1^\pm} \simeq 207 \text{ GeV}, \quad M_{\chi_2^0} \simeq 203 \text{ GeV}, \quad M_{\chi_1^0} \simeq 107 \text{ GeV}. \quad (4.3)$$

Since the staus are heavy, a priori the preferred decay channel of χ_2^0 is through the lightest Higgs, $m_h = 126 \text{ GeV}$. However, since $M_{\chi_2} - M_{\chi_1} < m_h$, this channel is suppressed and the favourite decay-channel turns out to be through an on-shell Z . As mentioned above, the main background for this final-state topology is the SM production of a W/Z pair.

Fig. 4 shows the histogram corresponding to the variable E_T^v , considering the background plus the signal with a luminosity of 100/fb, which will be reached in the near future. The SUSY signal is clearly visible. The position of its peak can be used to extract information about the SUSY spectrum in the way discussed in sect. 3. More precisely, for this model the prediction of eq.(3.4) for the visible transverse energy at the pole of the signal is $\hat{E}_T^v|_{\text{pole}} \simeq 94 \text{ GeV}$, which is consistent with the bin of the histogram corresponding to the maximum signal, i.e. 90 – 110 GeV.

This case illustrates the possibility that the peak of the E_T^v -histogram for the signal lies close to the peak for the background, i.e. M_Z . Note from Fig. 4 that both peaks are at the same bin, as expected.

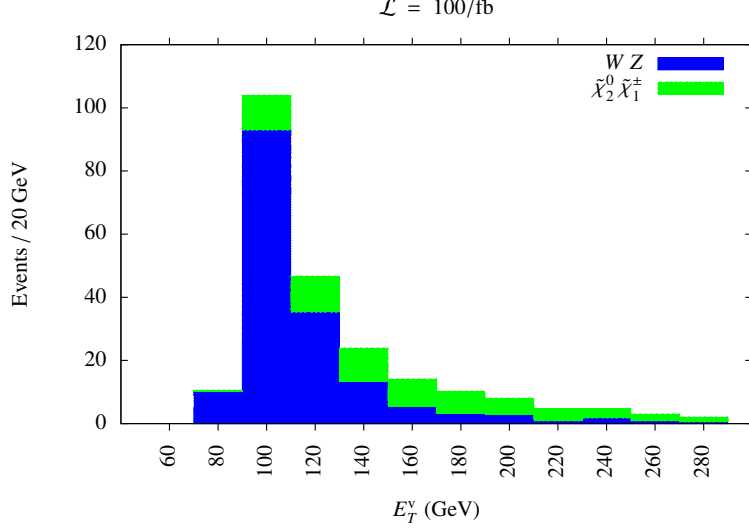


Figure 4: Histogram (in number of events) of E_T^v for the parameters corresponding to Model 1 (see text), taking into account the signal plus the dominant background (W/Z production).

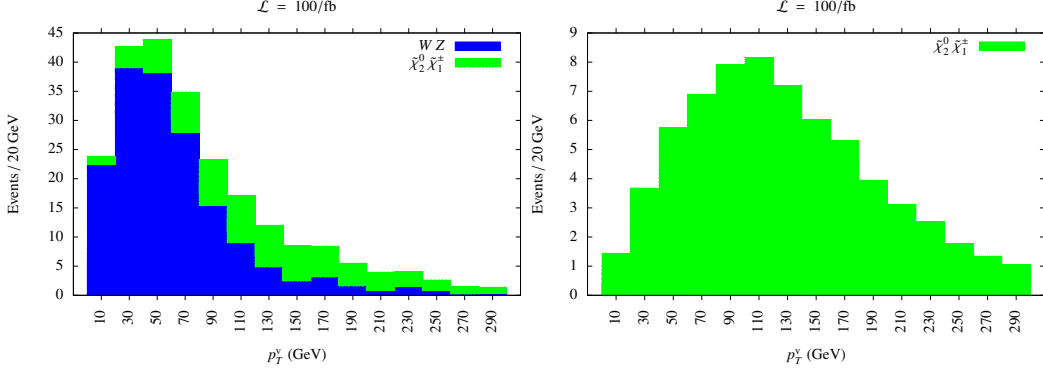


Figure 5: The same as in fig.4, but now the histogram is on the variable p_T^v for: left) background + signal, right) only signal.

As discussed at the end of sect. 3, this shortcoming can be improved by plotting p_T^v instead of E_T^v . The result is shown in fig.(5).

Although the improving is not dramatic, it is clearly visible. Note that the peak of the signal (the bin centered at 50 GeV) is now displaced with respect to the background one (the bin at 30 GeV). Fig.(5) shows just the p_T^v -histogram of just the signal events. Of course, it is not something one can realistically obtain from the experiment but we present it in order to show the shape of the signal events, gathered around the (theoretically predicted) maximum.

Model 2

In this case the relevant supersymmetric spectrum reads

$$M_{\chi_1^\pm} \simeq 273.5 \text{ GeV}, \quad M_{\chi_2^0} \simeq 273 \text{ GeV}, \quad M_{\chi_1^0} \simeq 53 \text{ GeV}. \quad (4.4)$$

χ_2^0 and χ_1^0 are almost pure bino and wino respectively. Now the decay of χ_2^0 through an

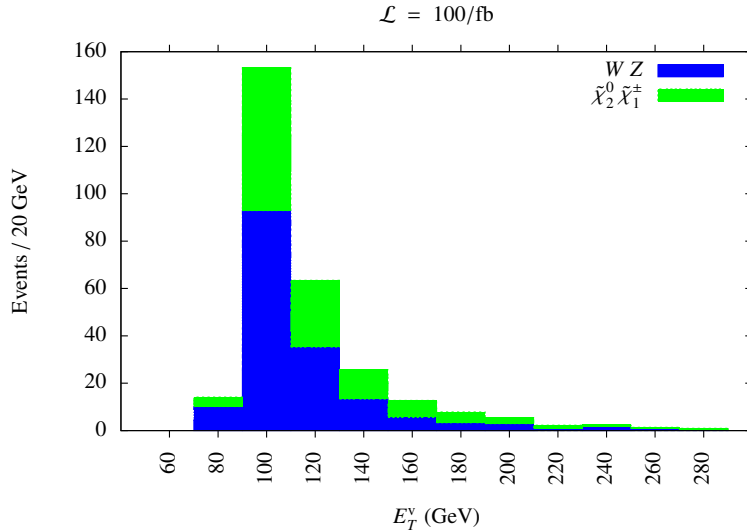


Figure 6: Histogram (in number of events) of E_T^v for the parameters corresponding to Model 2 (see text), taking into account the signal plus the dominant background (W/Z production).

on-shell Higgs is kinematically allowed, so one would expect it to be the preferred decay channel. However, the branching ratio of the decays through a Higgs or through a Z -boson are 39% and 61% respectively. The reason is the following. Due to the relatively high value of $\tan\beta$, the χ_2^0 and χ_1^0 neutralinos are essentially gauginos with a small \tilde{H}_d^0 component and a *very* small \tilde{H}_u^0 component. On the other hand, the physical Higgs-boson is essentially H_u^0 for the same reason. Then the χ_2^0 decay through a Higgs occurs thanks to those very small \tilde{H}_u^0 components and gets suppressed, while for the decay through a Z -boson may occur through the not-so-small \tilde{H}_d^0 components of the neutralinos.

Fig. 6 shows the histogram corresponding to the variable E_T^v , containing the background plus the signal, again with a luminosity of 100/fb. The SUSY signal is of course weaker than in Model 1, since the supersymmetric masses are larger. On the other hand, it is nice that now the peak of the signal does not coincide with the peak of the background anymore. In this case eq.(3.4) gives us $\hat{E}_T^v|_{\text{pole}} \simeq 146$ GeV, consistent with what the signal peak visible at Fig. 6.

As for Model 1, in this case the separation between the signal and background peaks is more efficiently achieved using the variable p_T^v rather than E_T^v , as it is shown in Fig. 7; however now the difference is more evident, as we expected.

Model 3

Finally, for Model 3 the spectrum reads

$$M_{\chi_1^\pm} \simeq 405.3 \text{ GeV}, \quad M_{\chi_2^0} \simeq 405.3 \text{ GeV}, \quad M_{\chi_1^0} \simeq 94 \text{ GeV}. \quad (4.5)$$

Again here χ_2^0 and χ_1^0 are almost purely wino and bino respectively, with very small Higgsino components of $\mathcal{O}(\lesssim 10^{-2})$. Also in this case the neutralinos contain much more \tilde{H}_d^0 than \tilde{H}_u^0 , leading to branching ratios $\text{BR}(\chi_2^0 \rightarrow \chi_1^0 h)$ and $\text{BR}(\chi_2^0 \rightarrow \chi_1^0 Z)$ to be 4% and 96%

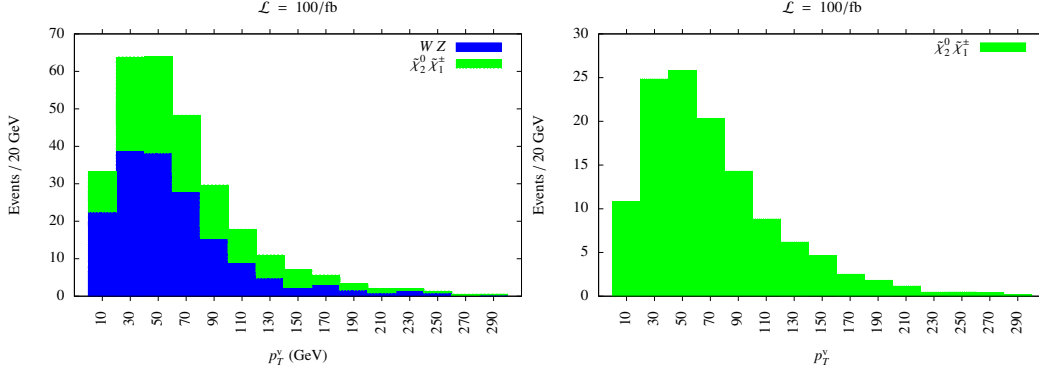


Figure 7: The same as in fig.6, but now the histogram is on the variable p_T^ν for: left) background + signal, right) only signal.

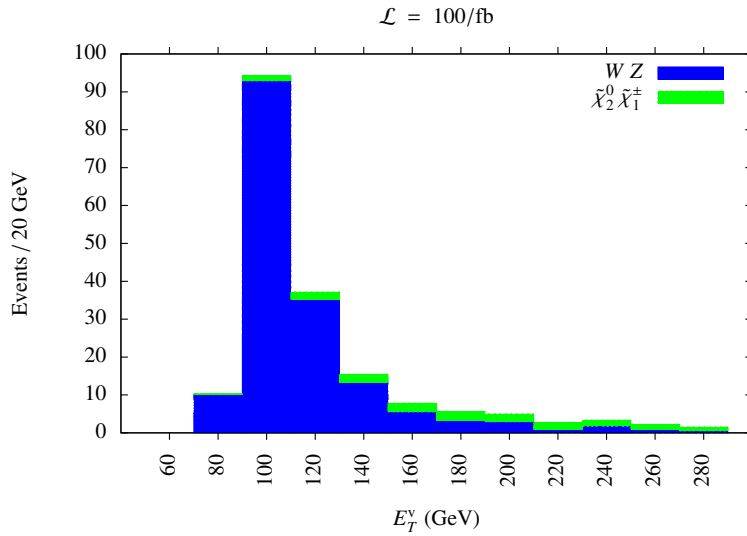


Figure 8: Histogram (in number of events) of E_T^ν for the parameters corresponding to Model 3 (see text), taking into account the signal plus the dominant background (W/Z production).

respectively, for similar reasons as before. Since now $\tan \beta$ is much larger the Higgs channel is even more suppressed.

Fig. 8 and Fig. 9 show the histograms in the E_T^ν and the p_T^ν variables respectively. They show similar features as for Model 2. The difference of course is that the signal is now quite small due the large supersymmetric masses. Still it is visible, especially for the p_T^ν variable. Since the S/B ratio is quite good the signal would be clear with larger luminosities (say 300/fb).

5. Conclusions

The study of chargino-neutralino pair production at the LHC finds nowadays an unprecedented motivation, since the detection of those particles could well represent the best (maybe unique) hope of discovering supersymmetry at the LHC. Different strategies have

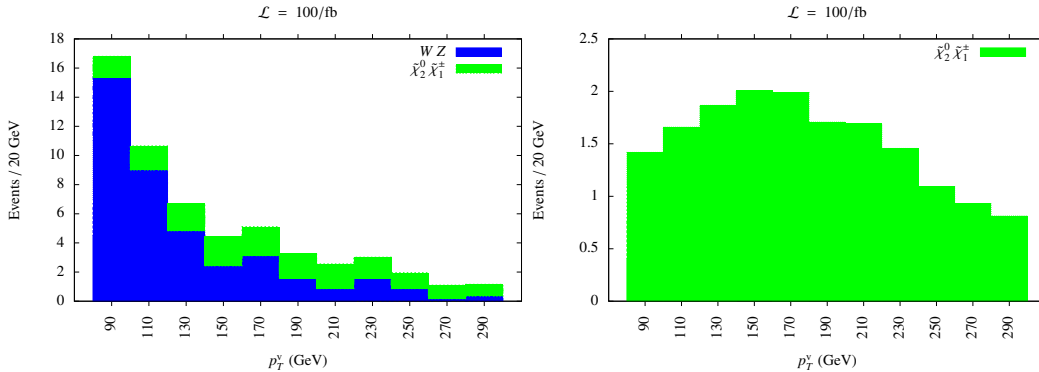


Figure 9: The same as in fig.8, but now the histogram is on the variable p_T^v for: left) background + signal, right) only signal.

been used so far by the experimental groups ATLAS and CMS to explore this process. They have been mainly focused on the analysis of 3-leptons plus missing-energy final states using standard kinematical variables, such as p_T and the invariant mass $m_{\ell+\ell^-}$. Most of the previous analyses either do not provide direct information about the relevant SUSY spectrum or are quite inefficient due to poor statistics as they make use of end-points in certain variables. In addition, they are designed to work for specific channels of decay (through sleptons or Z -boson).

In this work, we have presented a new -purely kinematical- method based on the variable E_T^v (visible transverse energy) which presents some very useful features. First of all, the histogram in E_T^v (in the frame where the decaying neutralino is at rest) has a pole. This translates into peaks in the actual experimental distributions and, consequently, is pretty robust against poor statistics. In addition, this concentration of signal-events around the maximum does not occur for the background-events, thus improving the S/B ratio and the discovery potential of new physics. Finally, the peak is correlated in a well-defined way to a precise combination of SUSY masses, namely

$$E_T^v|_{\text{pole}} = \frac{1}{2M_{\chi_2^0}} [M_{\chi_2^0}^2 - M_{\chi_1^0}^2 + M_v^2] \quad (5.1)$$

where $M_{\chi_2^0}$, $M_{\chi_1^0}$ and M_v are the masses of the decaying neutralino χ_2^0 , the lightest neutralino (LSP) and the visible system to which χ_2^0 decays to (typically two leptons or two b-jets).

Of course, when passing from the CM to the LAB system the maximum becomes less sharp and the position of the maximum is slightly shifted. However, these effects are not dramatic and, besides, can be well estimated in a semi-analytical way and kept under control.

We have illustrated these facts performing a realistic analysis of particular SUSY models, where the χ_2^0 neutralino decays mainly through a Z boson. We have focussed in events where the final state consists of 3 leptons plus missing energy, showing that the SUSY signal in the E_T^v variable could be very well detected at the LHC running with 14 TeV and a luminosity of 100/fb, which is attainable in the near future.

Let us finally stress that the same method can be applied to any possible decay channel of χ_2^0 : through squark, sleptons or a Higgs. The latter case is actually the most frequent one for MSSM models. Then, the most probable final state contains 2 b-jets, 1 lepton (or jet) and missing energy. The $h \rightarrow b\bar{b}$ channel has the additional advantage of having large branching ratios compared to the $Z \rightarrow \ell\bar{\ell}$ case. On the other hand, the topology $j_b j_b \ell$ is much less clean and difficult to reconstruct properly. Thus it requires a separate study which is out of the scope of the present paper and will be the subject of a future research work.

Acknowledgements

We are grateful to Krzysztof Rolbiecki for very useful discussions. This work has been partially supported by the MICINN, Spain, under contract FPA2010-17747; Consolider-Ingenio PAU CSD2007-00060, CPAN CSD2007-00042. We thank as well the Comunidad de Madrid through Proyecto HEPHACOS S2009/ESP-1473 and the European Commission under contract PITN-GA-2009-237920. M. E. Cabrera acknowledges the financial support of the CSIC through a predoctoral research grant (JAEPRe 07 00020); and the ERC “WIMPs Kairos - the moment of truth for wimp dark matter” (P.I. Gianfranco Bertone). The work of A. Casas has been partially supported by the MICINN, Spain, under contract FPA2010-17747 and the Consolider-Ingenio PAU CSD2007-00060, CPAN CSD2007-00042. We thank as well the Comunidad de Madrid through Proyecto HEPHACOS S2009/ESP-1473 and the European Commission under contract PITN-GA- 2009-237920.

References

- [1] F. Gianotti, *Update on the Standard Model Higgs searches in ATLAS*, [ATLAS-CONF-2012-093](#).
- [2] J. Incandela, *Update on the Standard Model Higgs searches in CMS*, [CMS-PAS-HIG-12-020](#).
- [3] **ATLAS Collaboration** Collaboration, G. Aad et al., *Search for supersymmetry in events with three leptons and missing transverse momentum in $\sqrt{s} = 7$ TeV pp collisions with the ATLAS detector*, *Phys.Rev.Lett.* **108** (2012) 261804, [[arXiv:1204.5638](#)].
- [4] **CMS Collaboration** Collaboration, S. Chatrchyan et al., *Search for electroweak production of charginos and neutralinos using leptonic final states in pp collisions at $\sqrt{s} = 7$ TeV*, *JHEP* (2012) [[arXiv:1209.6620](#)].
- [5] **ATLAS Collaboration** Collaboration, G. Aad et al., *Expected Performance of the ATLAS Experiment - Detector, Trigger and Physics*, [arXiv:0901.0512](#).
- [6] M. E. Cabrera and J. A. Casas, *Understanding and improving the Effective Mass for LHC searches*, [arXiv:1207.0435](#).
- [7] A. Djouadi, J.-L. Kneur, and G. Moultaka, *SuSpect: A Fortran code for the supersymmetric and Higgs particle spectrum in the MSSM*, *Comput.Phys.Commun.* **176** (2007) 426–455, [[hep-ph/0211331](#)].
- [8] M. Muhlleitner, A. Djouadi, and Y. Mambrini, *SDECAY: A Fortran code for the decays of the supersymmetric particles in the MSSM*, *Comput.Phys.Commun.* **168** (2005) 46–70, [[hep-ph/0311167](#)].

- [9] A. Djouadi, J. Kalinowski, and M. Spira, *HDECAY: A Program for Higgs boson decays in the standard model and its supersymmetric extension*, *Comput.Phys.Commun.* **108** (1998) 56–74, [[hep-ph/9704448](#)].
- [10] A. Djouadi, M. Muhlleitner, and M. Spira, *Decays of supersymmetric particles: The Program SUSY-HIT (SUspect-SdecaY-Hdecay-InTerface)*, *Acta Phys.Polon.* **B38** (2007) 635–644, [[hep-ph/0609292](#)].
- [11] B. Allanach, *SOFTSUSY: a program for calculating supersymmetric spectra*, *Comput.Phys.Commun.* **143** (2002) 305–331, [[hep-ph/0104145](#)].
- [12] J. Alwall, M. Herquet, F. Maltoni, O. Mattelaer, and T. Stelzer, *MadGraph 5 : Going Beyond*, *JHEP* **1106** (2011) 128, [[arXiv:1106.0522](#)].
- [13] T. Sjostrand, S. Mrenna, and P. Z. Skands, *PYTHIA 6.4 Physics and Manual*, *JHEP* **0605** (2006) 026, [[hep-ph/0603175](#)].